DOI: 10.26599/FSHW.2025.9250813

Contents lists available at SciOpen

Food Science and Human Wellness

journal homepage: https://www.sciopen.com/journal/2097-0765

China Food Publishing Co.

Tissue structure and nutritional composition of tree peony (*Paeonia suffruticosa* Andr.) seed during germination and evaluation of lipid concomitants of the oils

Xiaoqing Xie[1], Hongyu Tang[1], Qingbin Lin[2], Jie Qiang[3], Yongsheng Cao[3],Yiting Duan[1], Yuan Gao[1], Siyu Zhang[1], Xiuzhu Yu[1]*

[1]*Shaanxi Union Research Center of University and Enterprise for Functional Oil Engineering Technology, College of Food Science and Engineering, Northwest A&F University, 22 Xinong Road, Yangling, 712100, Shaanxi, P. R.China*

[2]*Shaanxi Heyang Chinese-funded Guoye Biotechnology Co., Ltd, Heyang, 715300, Shaanxi, P. R.China*

[3]*Shaanxi Guanzhongyoufang Oil Co., Ltd, Baoji, 721000, Shaanxi, P.R. China*

ABSTRACT: Germination as flexible pretreatment enhances oilseed processing. This study investigated whether germination changes the structure and processing performance of tree peony seed (TPS). Structurally, the number and fiber structure of oil bodies were increased and became more visible, and oil was more easily extracted after germinated. And sugars, proteins and lipids are main metabolic sequences of energy substances in TPS. Germination increased TPS's internal water freedom, causing total sugar content to rise initially and then decrease, while protein and oil contents peaked on 15 d at 24.02 g/100 g and 57 g/100 g, respectively. Moreover, glycerolipids and glycerophospholipids dominated the lipid metabolites of TPS, and germinated alter the expression of Diglyceride, Triglyceride, and Phosphatidylcholine. Tree peony seed oil exhibited elevated lipid concatenation post-germination, boasting 4130.74 mg/kg of phytosterols and 94.68% unsaturated fatty acids. Consequently, moderate germination enhanced the nutritional quality of TPS, with a 15-day germination period being optimal for its application as an oilseed in the production of superior nutritious oils.

Keywords: Tree peony seed; Germination; Structure; Lipid concomitant.

1. Introduction

Within the family Paeoniaceae and genus Paeonia, the tree peony (*Paeonia suffruticosa* Andr.) is a significant national resource plant, cultivated and utilised for over 2,000 years, with substantial market potential in China [1]. In recent years, the tree peony has attracted attention not solely for its aesthetic appeal but additionally for its potential as a source of valuable bioactive compounds [2]. The roots and various organs of the tree peony are rich in salvinorin, paeoniflorin, phytosterol, and other constituents with significant medicinal properties. Additionally, tree peony seed (TPS) has an oil content ranging from 8.66% to 24.65%, with more than 88.62% comprising unsaturated fatty acids, including 72.83% α-linolenic acid [3]. Therefore, TPS was a impeccable source for providing healthy and high-quality edible vegetable oils

***Corresponding author**
xiuzhuyu@nwafu.edu.cn

Received 2 January 2025
Received in revised from 9 February 2025
Accepted 2 July 2025

compared to other oilseed crops and tree peony seed oil (TPSO) were declared a new resource food by the Ministry of Health of the People's Republic of China in 2011 [4].

Seed germination, employed as a technique in food bioprocessing, involves the prompt transition of mature seeds from a state of dormancy to a state of emergence. Then subsequently activates the corresponding basal metabolism to supply the essential resources for seedling development [5]. Thus, the capability of germination to rapidly and effectively improve the tissue structure, nutritional qualities, and functionality of oilseeds without the production of harmful derivatives has recently attracted the interest of a wide range of researchers [6]. As a result, the germination of oilseeds resources plays a critical role in the Chinese functionalized oil processing, as well as the nation's exploitation of related oil products. As evidenced by Ohanenye [7], germination improves the dietary benefits of oilseeds through boosting the protein digestibility of legume seeds and expanding there physiological attributes by inhibiting the action of trypsin inhibitors. Additionally, Gan [8] have also discovered that germination promotes the accumulation of bioactive constituents such as vitamins, polyphenols and phytosterols through the resynthesis of secondary metabolites. Meanwhile, the process of germination eliminates toxic, harmful and anti-nutritional substances from oilseeds, facilitating the efficient production of nutritious, highly digestible edible oils [9]. While much is known about the benefits of germination in various oilseeds, limited research has focused on its effects on TPS and TPSO derived from it. In particular, there has been no exploration into whether germination can improve the functional properties of TPS and TPSO by modifying tissue structure, moisture content, or nutritional composition. Given the unique composition of TPS and its potential for providing a high-quality edible oil, investigating how germination influences the internal growth state, tissue structure, oil body structure, and nutrient composition of TPS could provide valuable insights into improving the oil's physicochemical and functional qualities.

In this study, we hypothesized that the tissue structure, moisture state of existence and nutritional composition of TPS could be altered by moderate germination, thereby improving the physicochemical properties and further enhancing the functional quality characteristics of TPSO. Hence, we investigated the alterations in internal growth state, tissue structure, oil body structure, lipidomics analysis, and nutrient composition of TPS throughout the germination to confirm our hypothesis. Furthermore, we prepared germinated TPSO by utilizing TPS at the ideal germination phase and evaluated alterations in the concentration of trace elements like tocopherols, phytosterols, and fatty acids. This study combines extensive research on the germination of TPS with an examination of the beneficial features of TPSO. Additionally, it serves as a theoretical framework for the creation of a moderating, effective, and environmentally friendly TPSO pretreatment method.

2. Materials and methods

2.1. Materials

The TPS and CTPSO (commmercial tree peony seed oil) were provided by Shaanxi National Industry Biotechnology Co., Ltd (Shaanxi, China). All fatty acid, tocopherol and sterol standards were purchased from

Sigma-Aldrich Corp (St. Louis, MO, USA). All pre-treatment reagents such as hexane, methanol, and dichloromethane were of analytical grade and purchased from Tianjin Kermel Chemical Reagent Co., Ltd (Tianjin, China).

2.2. Seed viability test of tree peony seed

Seed viability assessment was determined by testing according to the methods of the International Seed Testing Association (ISTA, 1985). As a control, 50 TPS with intact particles that had been pre-treated with boiling water for 10 minutes to eliminate viability were chosen. Then, the TPS was immersed in 200 mL of deionized water, incubated at 30 ◦C for 4 h stained with 0.5% (w/v) triphenyltetrazolium Chloride (TTC) aqueous solution, and finally assayed after being kept in the dark at 30 ◦C for 4 h to observe the color change.

2.3. Germination of tree peony seed

The methods of seed germination and physical parameters used including temperature and humidity are referred to Ren [10]. The TPS was washed with deionized water and soaked overnight in 100 mg/L of GA3 at 30 ◦C to break dormancy and promote germination, after draining the soaking water, the seeds were placed in the germination chamber. The TPS was placed on filter paper moistened with deionized water at germination in a constant climate chamber (HWS-450, Ningbo Southeast Instrument Co., LTD, China) with a temperature of 25 ◦C and a relative humidity of 80%. Deionised water at a concentration of 30% (by seed weight) was uniformly sprayed, and after the TPS absorbed the water (approximately 3 h), additional water was sprayed at moderate intervals of every 12 h at a dosage equivalent to 15% of the seed's dry weight to ensure adequate water absorption during germination. After germination, the TPS was dried in the air oven (DHG-9140A, Jinghong experimental equiprabender GmbH & Co. KG, China) at 40 ℃ for 24 h and then manually shelled. To guarantee the precision of ensuing correlation measurements, TPS were gathered at the same time of every 3 d.

In this study, the groups were named as follows: prepared by germinated with 3 d, 6 d, 9 d, 12 d, 15 d, 18 d, and 21 d were recorded as GTP3, GTP6, GTP9, GTP12, GTP15, GTP18 and GTP 21. Besides, the TP was prepared from the original TPS used as the control group.

2.4. LF-NMR transverse relaxation time measurement

Referring to the method of Cheng [11], an Low-Field Nuclear Magnetic Resonance (LF-NMR) analyzer (NMI20-015V-I, Suzhou Niumag Analytical Instrument Co., China) fitted with a 0.5 T permanent magnet, which corresponds to a proton resonance frequency of 23.1 MHz at 32 ℃, was used to evaluate transverse relaxation time (T2). The TPS was put inside a 15 mm diameter cylindrical glass tube. The carr–purcell–meibum–gill (CPMG) sequence was used to detect the T2 of the TPS, and the T2 relaxation spectra of the TPS were obtained after inversion, including the relaxation time and the corresponding amount of relaxation signal. The precise parameters of the experiment were as follows: The cumulative sampling number (NS) was established at 8, the hard pulse 90° pulse width (P1) was designated as 14 μs, the repeated sampling waiting time (TW) was set to 1000 ms, the number of echoes (NECH) was fixed at

15,000, the start time was 0.01 ms, the number of iterations was determined to be 10,000, and the cut-off time was established at 10,000 ms.

2.5. Magnetic resonance imaging analysis

The LF-NMR analyzer frequency coil at 32 ℃ was used to obtain the Magnetic resonance imaging (MRI). Proton density images of the TPS was acquired using the multiple spinechoes (MSE) sequence of MRI software. The following scanning protocols were used: field of view (FOV) = 70 mm ×70 mm, average = 16, read size = 256, phase size = 192, echo time (TE) of 10 ms, and repetition time (TR) of 800 ms.

2.6. Scanning electron microscopy analysis of tree peony seed

Glutaraldehyde fixation at 4 ℃ and dehydration with alcohol to preserve the TPS tissue. Then TPS was cut into 5 mm × 5 mm cross-sections and attached to the copper sheet with conductive adhesive, then sprayed with gold using an automated sputter gold plating machine following the method of Fu [12]. The morphological characteristics of the TPS was examined using scanning electron microscopy (SEM) (Nano SEM-450, FEI Ltd., Czech Republic) at an accelerating voltage of 5 kV, with images captured at 1500 × magnification.

2.7. Confocal laser scanning micrographs analysis of tree peony seed

The microstructure of oil bodies in TPS was observed using confocal laser scanning micrographs (CLSM) (Leica TCS SP8, Leica Microsystems, Germany) and a 63 mm oil immersion objective. The TPS was sliced with a freezing microtome (CM1860, Leica Biosystems Nussloch GmbH, Germany) and the thickness of the slices was 20 μm. Then, the lipids were stained separately using Nile Red (1 mg/mL acetone) according to the staining protocol described by Garcia [13]. The detailed procedure was as follows: Position the cut TPS section on a slide, apply the prepared Nile red solution in a dark environment for 10 min, subsequently rinse with sterile water to eliminate excess dye, and cover with a coverslip for examination. Then observed and photographed at an excitation wavelength of 552 nm with a 40 × objective lens.

2.8. Determination of the nutritional composition of tree peony seed

The Association of Official Analytical Chemists' established official procedures (AOAC, 2005) were used to determine the protein content (979.09) of TPS. Oil and water content as detected by CPMG sequence of LF-NMR. The 3,5 dinitro salicylic acid method was used for the determination of the content of total and reducing sugar.

2.9. Lipidomic analysis of tree peony seed

Six samples were randomly selected in TP and GTP15 groups, and lipid profiling was performed using ultrahigh-performance liquid chromatography coupled with a Q Exactive mass spectrometer (UPLC-Q Exactive MS) (Thermo Fisher Scientific, Waltham, MA, USA) for high-throughput lipidomics determination. The metabolites were extracted by suspending 50 mg of finely ground TPS in a 400 μL solution of methanol and deionized water (1:1, v/v), with the addition of 0.02 mg/mL of L-2-chlorophenylalanine as an internal standard. The mixture underwent high-throughput frozen tissue milling at -10 ℃, followed by sonication at 40

kHz for 30 min at 5 ℃ and incubation at -20 ℃ for 30 min to induce protein precipitation. Subsequently, the samples were centrifuged at 13,000 g for 15 min at 4 ℃ to collect the supernatant, then filtered through a 0.22 μm pore size membrane and transferred into liquid chromatography bottles for analysis. The UPLC-Q Exactive MS analysis was referred to the method of Dong [14].

2.10. Preparation of tree peony seed oil

Hull-less TPS was ground in a precision laboratory mill (Quadrumat Junior 880110, Brabender GmbH & Co. KG, Germany) and sifted through 40 mesh to obtain TPS flour. Petroleum ether was used as the extraction agent in the ultrasonic-assisted extraction process to prepare crude TPSO. The supernatant was extracted after centrifugation at 8000 r/min for 10 min, and the reagent and TPSO were separated using a rotary evaporator. Then TPSO was sealed and stored at 4 ℃ for further testing. In this study's classification, the TPSO derived from ungerminated TPS was designated as TPSO-0, while the tree peony seed oil extracted after 15 days of germination was named TPSO-15. In addition, CTPSO was also a product prepared using cold pressing technology, which serves as a comparative reference in this experiment.

2.11. Fatty acids analysis of tree peony seed oil

The fatty acids were quantified as methyl esters utilising the method delineated by Wang [15], employing a gas chromatograph (GC) (Agilent 6890N, Agilent Technologies, USA) fitted with an HP-INNOWAX capillary column (0.25 mm, 30.0 m × 0.25 mm). Weigh out 0.1 g of TPSO, add 2 mL of petroleum ether-ether solution (2:1, v/v), and shake to dissolve the oil. Next, add 1mL of KOH-methanol solution (2%, w/v), shake for 3 min allow the mixture to stand at room temperature for 2 h.

Following volume fixation, 1.0 mL supernatant was extracted and utilized for GC analysis. The program's temperature inc rease was 50 ℃ for 5 min, then 10 ℃/min to 230 ℃, which was maintained for 20 min, the inlet port was 250 ℃ and the hydrogen flame ionization detector detection port temperature was 270 ℃.

2.12. Tocopherols analysis of tree peony seed oil

The procedure used to determine the tocopherol content of TPSO was modified from that described by Wang [15]. 1.0 mL of TPSO was accurately weighed into a 2 mL brown volumetric flask, combined with n-hexane using a vortex mixer, filtering the mixture through a 0.22 μm organic filter membrane, and then analyzing using high-performance liquid chromatography (HPLC). The HPLC (LC-20AT, Shimadzu, Japan) is equipped with a PDA detector and a CNW Athena silica column (250 mm × 4.6 mm, 5 μm, CNW, Germany). And, the injection volume was 10 μL, and the mobile phase was n-hexane: isopropanol (98.5:1.5, v/v) at a flow rate of 1 mL min^{-1}. Tocopherol was detected at a wavelength of 295 nm, and the results were quantified by the external standard method and expressed as mg/kg.

2.13. Phytosterols analysis of tree peony seed oil

The phytosterols in the TPSO was essentially extracted in the following way, according Wang [16]'s report. After pretreatment, 1.0 μL of the TPSO was analyzed in the gas chromatograph-mass spectrometer

(GC-MS) (QP2010, Shimadzu, Japan) equipped with a SH-Rxi-5Sil MS capillary column (30 m × 0.25 mm × 0.25 μm, Shimadzu, Japan). Analysis was carried out using the following program: the column temperature is maintained at 40 ℃ for 3 min, then warmed up to 120 ℃ at 4 ℃/min and 240 ℃ at 6 ℃/min held for 12 min. The solvent was kept back for 10 min, With a partition ratio of 80:1, a carrier gas of helium flowing at a rate of 0.7 mL/min, a scan period of 0.5 s, and a mass range of 50~650 m/z. The data were expressed in mg/kg using the internal standard method.

2.14. Statistical analyses

All experiments were performed with at least three replicate measurements unless otherwise stated, and the data were indicated as mean ± standard deviations (SD). The significant changes among the samples were estimated with ANOVA using Turkey's multiple comparison test to a 5% level of significance, using the software SPSS 20.0 (SPSS, IBM, USA). Figures were created by GraphPad Prism 8.0 (GraphPad, San Diego, USA).

3. Results and discussion

3.1. Seed viability test and evaluation of tree peony seed

Assessing initial seed viability is crucial for evaluating seed germination potential and requirements [17]. Viable seed embryos engage in redox reactions during respiration and exhibit a red hue. In this experiment, TPS was dehydrogenated and reduced to a red color by triphenyl methyl (Figure S1). In contrast, the boiled TPS was completely devitalised and had no change in colour. Thus, this research avoided the influence of TPS viability.

3.2. Moisture state and H protons migration behavior of tree peony seed

T2 relaxation curve describes the mobility and distribution of H protons inside the seed sample, which accurately represents the variation of state and migration behavior [18]. The water content is reflected in the T2 relaxation spectrum's peak area, where a larger peak area indicates more water in that state. Besides, in the T2 relaxation spectrum, T_{21} in the range of 0.1-10 ms is defined as bound water associated with cellular binding to organisms. The 10 to 100 ms T_{22}, on the other hand, is thought to be immobilized water existing in the intercellular. Furthermore, the T_{23}, which indicates the presence of free-flowing water both intracellularly and extracellularly, occurs within a time frame of 100 to 1000 ms [19]. The relaxation time distribution curves of TPS germinated were displayed in Fig.1, which revealed four distinct distribution regions, suggesting the existence of multiple states of water in the TPS. It's widely recognized that H protons have longer T2 relaxation times at higher flow rates [20]. In this research, T_{21} of all TPS groups were unremarkably altered during germination, with no intensive contact with external water, which was inassociated with morphological and structural alterations in the organism. On the other hand, T_{22}'s signal amplitude increased between 3-15 d after TPS germination (GTP3, GTP6, GTP9, GTP12 and GTP15), accompanied by a significant rightward shift of T_{23}, which peaked in GTP15. That might be due to more water existing in the cellular interstitial space, germination increased the internal water freedom of TPS, enhanced metabolic activities, and promoted

germination [21]. Following 18 and 21 days of TPS germination (GTP18 and GTP21), as the radicle tip approaches a stage conducive to penetrating the seed coat under restricted water availability, the peak areas of T_{22} and T_{23} diminish during the later stages of germination [20]. According to these findings, germination enhanced H proton mobility and permitted more water to enter TPS, GTP15 had the maximum mobility and was thought to be germination at the ideal period.

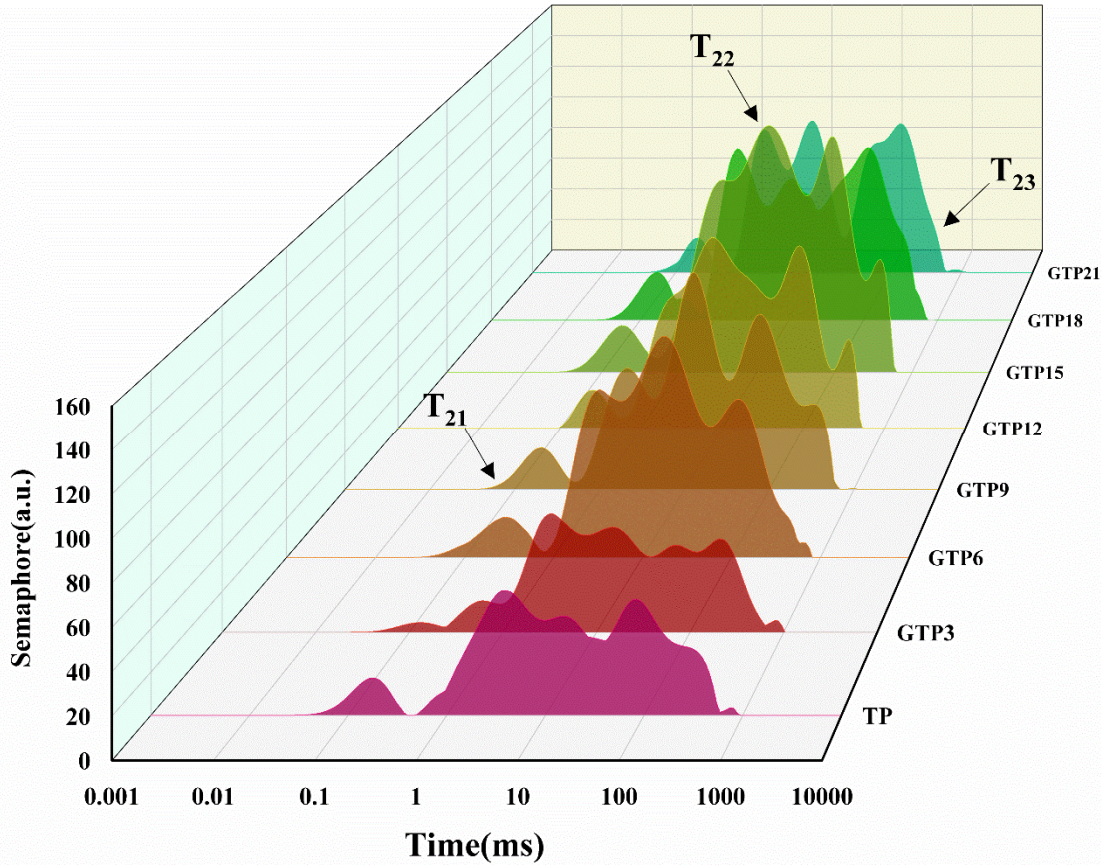

Fig. 1. T2 relaxation diagram of TPS during germination.

3.3. MRI analysis of water-oil content and dynamics in tree peony seed

In addition to analyzing LF-NMR signals, it is also possible to visualize the water-oil content and its associated dynamic processes through MRI observation [22]. The shades of colors in the H proton density-weighted plot directly represent the disparity in the amount of relaxation signals due to the different water contents, and can also reflect the law of water dynamics in TPS during germination [23]. In the MRI of TPS, red indicates areas of high H proton density, while green denotes areas of low H proton density. As shown in Fig. 2, the color tends to be more red the higher the moisture and number of H atoms. From the group of TP to GTP15, the TPS was continuously absorbing water and beginning to germinate, which explains whether the signal strength shows an upward trend with increasing red areas as germination time moves on. Subsequently, at the late stage of germination (GTP18 and GTP21), the TPS ceases water absorption, while simultaneously, internal metabolism intensifies, leading to a gradual increase in the activity of metabolism-related enzymes. Then seeds restart absorbing water during the growth period and cell cleavage and differentiation accelerate, the area of water distribution would continue expanding [24]. Consequently, this research demonstrates that the trend of the red area in the H proton density-weighted plot

corresponds to the degree of water uptake during TPS germination, which first rises, then falls, and then rises again. Among the groups, the GTP15 had the most H protons density intensity. Our study using LF-NMR analysis, systematically assessed the distribution of water states in TPS during the germination, which provided perspectives for understanding its physiological mechanisms.

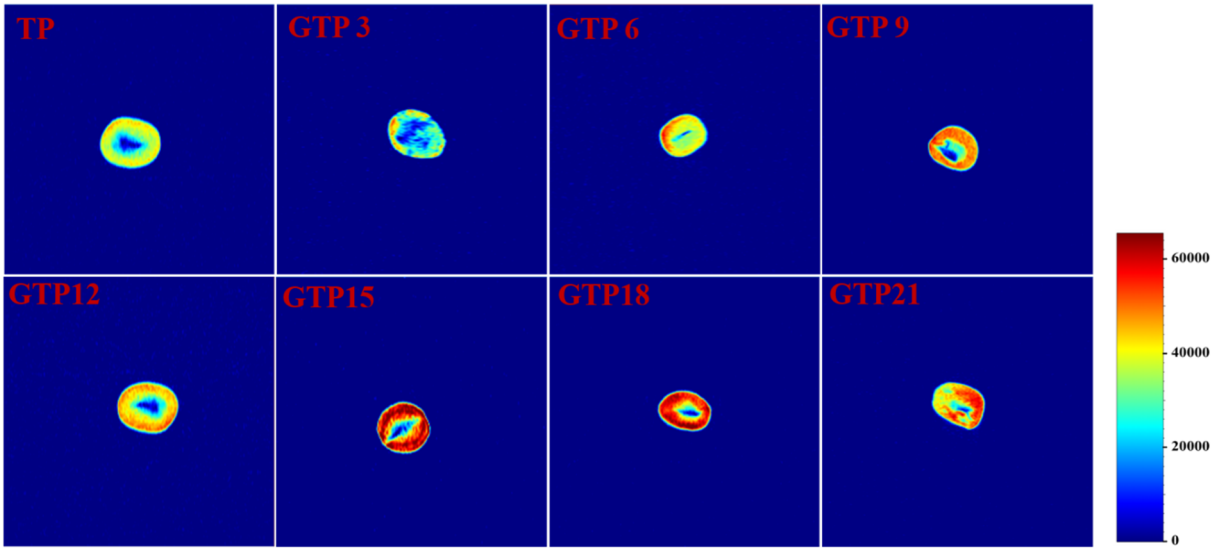

Fig. 2. T2 weighted MRI pseudo-color images of TPS during germination. The deeper the color, from blue to red, the stronger the signal.

3.4. Morphological characteristics of tree peony seed

The changes attributed to germination are reflected not only in the physical composition as well as in the microstructure of the seeds. Consequently, a more in-depth analysis of the morphology during germination is essential, with the findings illustrated in Fig. 3. Structurally, the increasing number and area of round or oval oil droplets (the red arrow) on the cross-section of TPS in 0–15 d of germination, which peaked in GTP15. In further, the particles present at the cross-section after germination were probably fibers of TPS encapsulated in the presence of lipids [25]. While the fiber structure indicates the protein matrix that encases and stabilises these oil bodies, potentially influencing the texture, stability, and quality of the oil throughout extraction and processing [26]. The fiber structure of TPS gradually became exposed in the later stages of germination, specifically at GTP18 and GTP21. This may occur because the oil was consumed as an energy source, thereby weakening the internal protein-oil-fiber bonds [27]. Therefore, the indentation of TPS after germination and the exposure of fiber structure indicate that the oil content in TPS was gradually released, this facilitates the extraction of TPSO. Nonetheless, an overabundance of germination leads to a gradual reduction in the oil necessary for organismal growth, rendering the processing of TPSO with elevated oil content less advantageous. Hence, TPS after 15 days germination was the most suitable raw materials for withdrawing and processing.

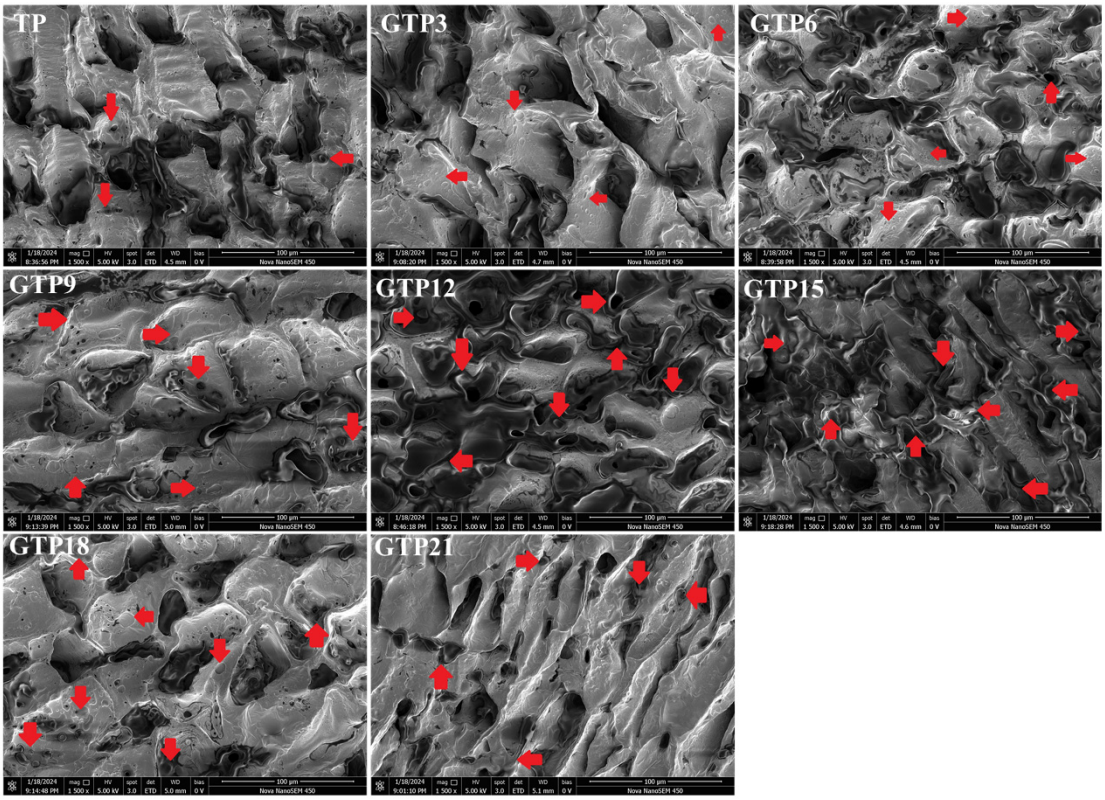

Fig. 3. Scanning electron micrographs of TPS cross-sections during germination

3.5. Oil structure observation of tree peony seed

The oil body stands as an organelle for storing lipids in plant seeds [28]. To further clarify the accumulation pattern of oil in TPS during germination, the dynamic changes of the oil body in the subcellular state were observed by CLSM. As demonstrated in Fig. 4, the oil bodies of TPS after germination showed a regular pattern from less to more in number, small to large, and sparse to dense in density under the fluorescence diagrams. A number of irregularly shaped oil bodies were observed in TP, whereas in GTP15, the oil bodies transitioned from an irregular shape to a rounded spherical form and were found to be the most prevalent. As germination progressed (GTP18 and GTP21), a subsequent reduction in the quantity of oil bodies occurred. Seed oil body was inversely proportional to oil body proteins, thus it can be surmised that the oil body proteins on the half-unit membranes of TPS were gradually hydrolyzed with the prolongation of germination [29]. Our study was similar to the results reported by Zhang [30] who argued that it showed a correlation between the increase in the volume of the oil body and its content was also positively related. Further, certain research has revealed that during germination, the phospholipid monomolecular layers containing little to no nucleosomal proteins fuse to form large oil bodies as the endoplasmic reticulum synthesizes an increasing number of small oil bodies [31]. The results observed by CLSM were consistent with the trends shown by the T2 relaxation curves and SEM, respectively, which all indicate that GTP15 was more suitable as a feedstock for the extraction of TPSO. Besides, subsequent studies are pending to further observe the oil body accumulation pattern of TPS under a transmission electron microscope.

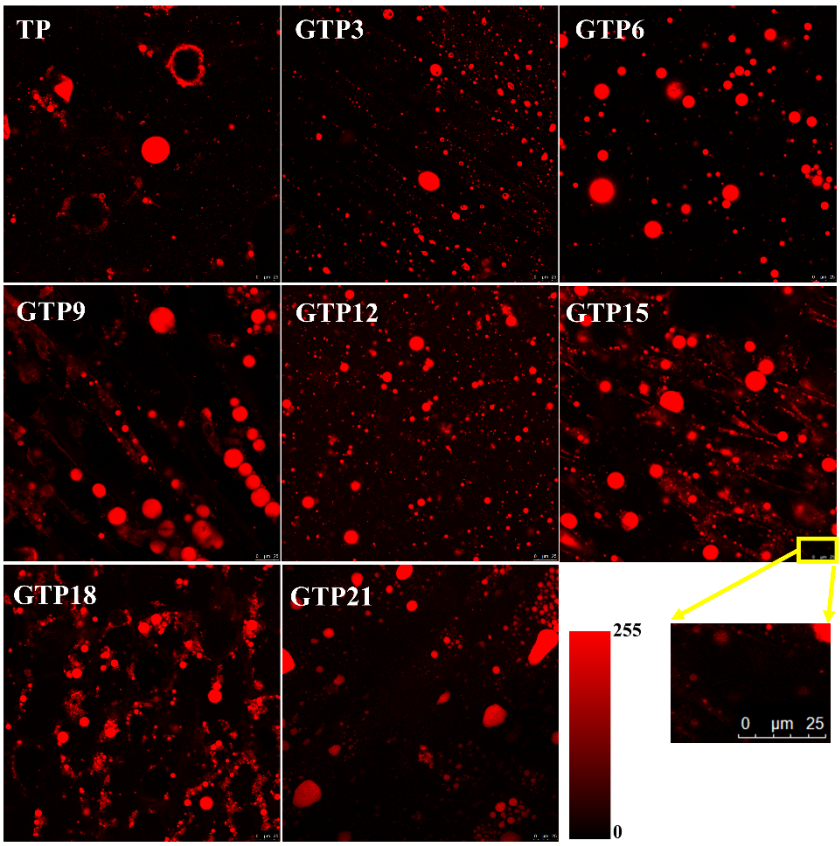

Fig. 4. Histochemical staining results in oil content of TPS during germination.

3.6 Nutritional composition of tree peony seed

The process of seed germination is mainly divided into the swelling, sprouting, germination, and seedling growth stages [32]. The breakdown and mobilisation of carbohydrates, lipids and proteins during the process of a seed emerging from dormancy and germinating assists this process. Additionally, which facilitates the formation of the cytoskeleton and the production of vital energy in growing plants [33]. The composition of nutrients of TPS during germination can be seen in Table 1. After germination, the moisture of TPS increased significantly from 9.11% (TP) to the maximum of 22.57% (GTP15), and then gradually decreased and stayed at about 19% ($P < 0.05$), indicating the rapid absorption of external water and the gradual increase in the internal water distribution area during the period of swelling [24]. Which was consistent with the results of 3.2 and 3.3 in this research, resulting in the increase of the signal intensity firstly and then decreased. The movement of stored fat toward the embryo in the early stages of germination and subsequent aggregation, along with the detachment of protein-bound fats from tissues, may be the cause of the increasing trend of oil content fluctuation between 21.65-39.95% along with the seed germination in TPS ($P < 0.05$) [34]. Nevertheless, in the advanced stages, protein synthesis requires energy from the breakdown of fat during the growth process. As a consequence, a sharp decrease in oil content was observed in GTP18/GTP21. After germination, the protein content of TPS increased significantly from 20.65% to 24.72% and reached a peak in GTP12, then followed by a gradual decrease in the trend ($P < 0.05$). The observed consequence would be explained by the protein stored during germination being synthesized in the form of amino acids and protein synthesis and used as a resource for energy and material metabolism

afterward [35]. In addition we observed that days to germination observed an inverse trend between reducing sugar content and total sugar content. The total sugar content in TPS dropped significantly ($P < 0.05$) during the first 12 days of germination, from the TP group to the GTP12. It is worth noting that although reducing sugar content showed an increasing trend from TP to GTP18 (from 3.73% to 4.26%) ($P < 0.05$), this does not contradict the fact that carbohydrates were the first to be metabolized. Instead, this trend reflects the biochemical process in which polysaccharides and starch are enzymatically hydrolyzed into smaller sugar molecules, such as reducing sugars, during the early stages of germination [36]. Accompanied by the accelerated decomposition of starch and other substances, the metabolism of other storage substances in the seed also produces a certain amount of reducing sugar, resulting in a gradual increase in its content [7]. Which clearly indicates that total sugar was indeed the first macronutrient being consumed for energy and structural needs. Consequently, we propose that the metabolic sequence of energy substances in TPS during germination follows the order of carbohydrate, protein and lipid. Considering the preparation of oils with a high probability of health benefits, GTP12 and GTP15 deserve to be the superior options.

Table 1. Nutritional composition (g/100g) of TPS during germination

Sample	Moisture	Oil Content	Protein	Total sugar	Reducing sugar
TP	9.11 ± 0.22c	34.07 ± 1.81bc	20.65 ± 0.34c	31.20 ± 1.49a	3.73 ± 0.11b
GTP3	19.99 ± 0.59ab	37.22 ± 1.13ab	21.11 ± 0.05c	27.39 ± 0.66bc	3.78 ± 0.17b
GTP6	18.95 ± 0.32b	39.63 ± 2.06a	23.06+0.33b	27.73 ± 0.49bc	4.06 ± 0.12ab
GTP9	20.32 ± 1.39ab	38.80 ± 1.63a	24.18 ± 0.67ab	27.84 ± 0.38bc	3.81 ± 0.02b
GTP12	21.21 ± 0.83ab	32.07 ± 1.07c	24.72 ± 0.36a	26.75 ± 0.50c	3.90 ± 0.21b
GTP15	22.57 ± 1.31a	39.95 ± 1.36a	24.02 ± 0.23ab	30.15 ± 1.30ab	4.00 ± 0.09ab
GTP18	19.55 ± 1.28b	27.98 ± 0.78d	23.04 ± 0.59b	28.39 ± 0.60abc	4.26 ± 0.07a
GTP21	18.86 ± 0.99b	21.65 ± 1.12e	20.67 ± 0.66c	28.05 ± 1.61bc	3.95 ± 0.09ab

*The moisture was calculated on a dry basis.
Different superscript letters in the same column indicate significant differences ($P < 0.05$).
The experiments were performed with three replicate measurements, and the data were indicated as mean ± standard deviations (SD).

3.7. Lipidomic analysis of tree peony seed

To investigate the impact of germination on TPS using the lipidomic techniques, TP and GTP15 were chosen as samples based on the results of structural and nutritional changes. A large amount of metabolic data was calculated, which was frequently analysed using PCA and PLS-DA. PC1 and PC2 in PCA accounted for 40.5% and 26.0% of the total variance, respectively. The two components together contributed 66.5% (Fig. S2a), indicating a high degree of similarity between the TP and GTP15. In addition, the PLS-DA showed that Component 1 accounted for 44.1% of the variance, while Component 2 accounted for 19.2% of the variance (Fig. S2b). A noteworthy observation in Fig. S2c is the high discriminant test values (R^2=0.8088, Q2=-0.001) for the samples, indicating well-predictive performance in determining the differences. Correlation data between samples allow for the quantification and analysis of the extent of variation in metabolite composition and abundance between samples. Thus, TP and GTP15 had more comparable metabolic profiles and abundances (Fig. S2d).

As presented in Fig. 5(a), a total of 870 lipid molecules were isolated and characterized from TPS, classified as glycerolipids (GL), glycerophospholipids (GP), sphingolipids (SP), sterol lipids (ST), and fatty

acyls (ST). Among the number of lipids identified as each lipid subclass, 289 triglycerides (TG) were detected, which accounted for 33.22% of the total lipids, followed by ceramides (Cer) (11.38%) and phosphatidylmethanol (PMe) (7.93%). Additionally, as shown in Fig. 5(b), the classification of the degree of unsaturation in the lipid carbon chain within TPS was explained. The percentages of polyunsaturated fatty acyls (PUFA) and saturated fatty acyls (SFA) in TPS were 31.20% and 23.27%, respectively, followed by monounsaturated fatty acyls (MUFA), and odd-numbered fatty acyls (ODD), besides other types of lipids accounted for 8.44%. Therefore, TPS lipids represent an ideal raw material for the production of vegetable oils with high nutritional value due to the contain 48.34% carbon chain unsaturated fatty acids.

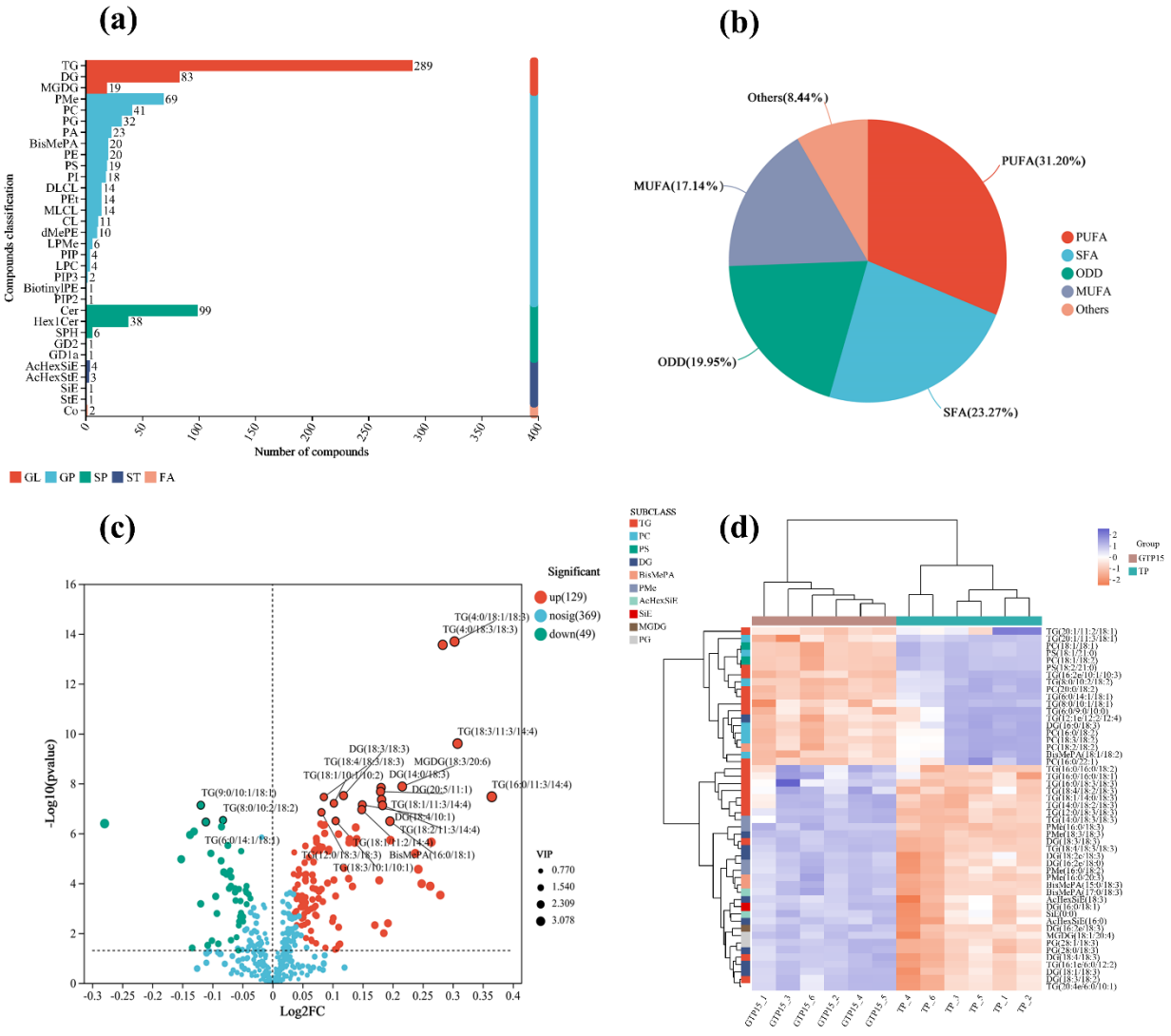

Fig 5. Lipid classification (a) and lipid carbon chain unsaturation classification (b) of TPS after germination. (c) Differential volcano plots of different lipid metabolites. The red and blue represent down- and up-regulated lipid metabolites, grey dots represent other metabolites that did not change significantly. (d) Heatmap showing Z score scaled the alteration of metabolites. The grid represents metabolites and the shade of the color indicates the relative level of the lipids. Blue and orange colors indicate increases and decreases in lipids, respectively, and white colors indicate no change.

The volcano plots (Fig. 5(c)) were used to display the differences in lipid metabolites. Fold Change (FC) ≥ 0.833 or ≤1.2, $P < 0.05$, representing down- and up-regulated lipid metabolites, and VIP ≥1, representing non-significant lipid metabolites of TPS. Of the 547 lipids identified, 178 were markedly altered. Among the differential lipid metabolites, 129 were up-regulated and 159 were down-regulated, a

detailed inspection revealed that triglyceride (TG) and diglyceride (DG), respectively, in agreement with previous studies TG and DG were the major differential lipid metabolites in germinating TPS [37]. Besides, hierarchical cluster analysis revealed a distinct clustering trend for TP and GTP15. For hierarchical cluster analysis, 50 differential lipids with VIP > 1.0 were chosen based on OPLS-DA in conjunction with one-way ANOVA ($P < 0.05$). The germinated TPS was easily distinguishable, as seen in Fig. 5(d). The primary distribution of differences was seen in the glycerol ester and phospholipid classes of TPS lipids, DG, TG, PS and PC [38]. These findings demonstrated that the germination was responsible for a number of GL (e.g., DG, TG) and GP(e.g., PC, PS, PMe and PG) modifications as well as the up-regulation of ST (e.g., AcHexSiE, SiE), providing valuable insights into metabolic processes that might be helpful for crop improvement and seed quality control in peonies. Nonetheless, further systematic lipidomic analyses are essential in future related studies.

3.8. Main fatty acid composition of tree peony seed oil

Essential nutrients and fatty acids serve as an effective source and store of energy, form the building blocks of cell structure, and function as biosynthetic intermediates for other critical biomolecules [39]. Therefore, accurate measurement of the main fatty acid content and composition in TPSO is crucial for quality control and evaluation. Table 2 shows remarkable differentials in the main fatty acids components in TPSO-0 and TPSO-15 ($P < 0.05$). The main fatty acids in all samples were palmitic acid, stearic acid, oleic acid, linoleic acid and linoleic acid. The lowest amount of unsaturated fatty acids (UFA) and polyunsaturated fatty acid (PUFAs) were found in CTPSO, which may be considering high temperatures during the refinement cause some UFA to break down. With the exception of palmitic acid, the content of all fatty acids increased significantly after 15 days of germination ($P < 0.05$). Besides, the contents of oleic acids and linolenic acids in the group of TPSO-15 were the maximum with 25.19% and 45.81%, respectively. After germinated, the UFA increased from 93.51% to 94.68%, while the saturated fatty acids (SFA) decreased by 1.17% ($P < 0.05$). It's worth noting that this coincides with the findings of Al-Taher & Nemzer [5] that the UFA increased as the seeds mature, and the opposite was true for SFA. This discrepancy between the amounts and ratios of the main fatty acids in TPSO in Table 2 and the amounts of fatty acids in TPS in Fig. 5(b) could be caused by the loss or modification of certain fatty acids during the extraction of TPSO because of things like solubility and thermal stability [40]. As well as by various pre-treatment and analytical techniques. Given that lipase activity in tissues determines fatty acid content [41], the germinating embryo of TPS may have the highest lipase activity during germination. The C1 and C3 glycerol bonds of triacylglycerols were subsequently hydrolyzed by the lipase enzyme to produce α-glycerophosphate and fatty acids [25]. Consequently, the fatty acid composition of TPSO has been altered by germination. It is evident that TPSO, which was made from TPS after germinated for 15 days, was a nutritious vegetable oil with a high content of PUFAs.

Table 2. Changes in the contents of main fatty acids of TPSO after germination

Fatty acid (%)	CTPSO	TPSO-0	TPSO-15
C16:0 (Palmitic acid)	5.58 ± 0.04a	5.34 ± 0.05b	4.16 ± 0.07c
C18:0 (Stearic acid)	1.20 ± 0.03a	1.14 ± 0.06b	1.16 ± 0.04b

C18:1 (Oleic acid)	25.13 ± 0.04a	24.42 ± 0.05b	25.19 ± 0.43a
C18:2 (Linoleic acid)	23.97 ± 0.04a	23.38 ± 0.06b	23.69 ± 0.30ab
C18:3 (Linolenic acid)	44.04 ± 0.10b	45.72 ± 0.04a	45.81 ± 0.15a
Saturated fatty acid (SFA)	6.79 ± 0.05a	6.49 ± 0.10b	5.32 ± 0.06c
Unsaturated fatty acids (UFA)	93.15 ± 0.05c	93.51 ± 0.10b	94.68 ± 0.06a
Polyunsaturated fatty acids (PUFAs)	68.02 ± 0.05b	69.09 ± 0.07a	69.49 ± 0.67a

* The CTPSO named for commercial tree peony seed oil, and TPSO-0 and TPSO-15 stand for the oil prepared from ungerminated TPS and germinated for 15 d TPS. Different superscript letters in the same column indicate significant differences ($P < 0.05$), and the data were indicated as mean ± standard deviations (SD).

3.9. Tocopherol Content of tree peony seed oil

Tocopherol is regarded as a necessary antioxidant compound that works in concert with polyphenols. Following germination, Table 3 demonstrated the tocopherol content of TPSO, with β-tocopherol not isolated due to its generally low amounts. The findings demonstrated that γ-tocopherol was substantially more prevalent in CTPSO, TPSO-15 and TPSO-0 than in δ- and α-tocopherol ($P < 0.05$). The CTPSO had a lower total-tocopherol content (303.77 mg/kg), while the TPSO-15 had the highest content of 350.26 mg/kg. Besides, the α-tocopherol grew gradually, rising from 12.34 mg/kg to 41.10 mg/kg after TPS post-germination. On the other hand, γ-tocopherol and δ-tocopherol in TPSO-0 exhibited a marginal decline, going from 332.09 mg/kg and 9.97 mg/kg to 301.04 mg/kg and 8.11 mg/kg in TPSO-15, respectively. However, the total tocopherol content in TPSO-0 and TPSO-15 had insignificant changes, these findings support the flaxseed germination research conducted by X et al [42]. More methyl groups are present in α-tocopherol than in other tocopherols [43]. According to our research, methylation of γ-tocopherol causes γ-tocopherols to change into α-tocopherols, which may have contributed to the rise in α-tocopherol of TPSO following germination. This was probably because isomer conversion occurs when γ-methyltransferase was activated during germination [44]. From a nutritional perspective, α-tocopherol acts as a fat-soluble antioxidant, protecting polyunsaturated fatty acids in cell membranes from oxidative damage and contributing to the prevention of cardiovascular and neurodegenerative diseases. Therefore, the germination-induced increase in α-tocopherol content may contribute to the improved nutritional value and oxidative stability of TPSO.

Table 3. The tocopherol content (mg/kg) of TPSO after germination

Tocopherol species	CTPSO	TPSO-0	TPSO-15
α-tocopherol	16.15 ± 0.60^{b}	12.34 ± 0.08^{c}	41.10 ± 1.28^{a}
γ-tocopherol	264.00 ± 1.54^{c}	332.09 ± 0.29^{a}	301.04 ± 0.61^{b}
δ-tocopherol	23.62 ± 0.30^{a}	9.97 ± 1.61^{b}	8.11 ± 0.96^{c}
Total-tocopherol	303.77 ± 1.84^{b}	354.41 ± 1.97^{a}	350.26 ± 0.29^{ab}

* The CTPSO named for commercial tree peony seed oil, and TPSO-0 and TPSO-15 stand for the oil prepared from ungerminated TPS and germinated for 15 d TPS. Different superscript letters in the same line indicate significant differences ($P < 0.05$), and the data were indicated as mean ± standard deviations (SD).

3.10. Phytosterol Content of tree peony seed oil

Being a fat-soluble substance, phytosterol's ability to maintain its stability at high temperatures enables oils to maximise its antioxidant properties [45]. The Table 4 displayed that CTPSO, TPSO-0, and TPSO-15 contained campesterol, stigmasterol, β-sitosterol, fucosterol, cycloartenol, and △ -5-avenasterol.

Specifically, there was an increase in β-sitosterol, fucosterol, and cycloartenol from TPSO-0 to TPSO-15, with respective amounts of 2374.13–2600.26 mg/kg, 947.63–985.06 mg/kg, and 274.89–279.06 mg/kg. Furthermore, lanosterol showed the lowest value of 30.07 mg/kg in TPSO-0. Additionally, the findings in our research indicated that germination substantially boosted the amount of total phytosterols in TPSO, specifically β-sitosterol and fucosterol, which increased by 267.37 mg/kg, 226.13 mg/kg, and 37.43 mg/kg, respectively ($P < 0.05$). Nevertheless, there was an insignificant change in the other phytosterol monomers after germination in TPSO ($P > 0.05$). The discoveries were consistent with those reported by Zhang et al. [44], who found that providing an appropriate germination treatment could increase the total phytosterols content in vegetable oil. This may be attributed to the accumulation of phytosterols during germination, which has been associated with enhanced antioxidant metabolism in previous studies [46]. Accordingly, this desired result may be utilized as a specific guide, which includes promoting aimed access to vegetable oils with high phytosterol and associated phytosterol monomer content through moderation germination.

Table 4. Changes in the contents of phytosterols (mg/kg) of TPSO after germination.

Phytosterol species	CTPSO	TPSO-0	TPSO-15
Campesterol	78.55 ± 3.00^{c}	80.91 ± 6.01^{b}	83.06 ± 1.78^{a}
Stigmasterol	42.18 ± 2.12^{b}	42.77 ± 3.47^{b}	47.06 ± 0.39^{a}
β-stiosterol	2124.01 ± 12.87^{c}	2374.13 ± 20.31^{b}	2600.26 ± 19.95^{a}
Fucosterol	903.87 ± 1.06^{c}	947.63 ± 18.14^{b}	985.06 ± 12.36^{a}
Lanosterol	32.46 ± 0.81^{ab}	30.07 ± 2.96^{b}	33.06 ± 5.88^{a}
△-5- Avenasterol	102.94 ± 2.77^{c}	112.98 ± 3.61^{b}	117.06 ± 10.06^{a}
Cycloartenol	205.49 ± 3.75^{b}	274.89 ± 0.96^{a}	279.06 ± 0.63^{a}
Total phytosterols	3489.51 ± 26.39^{c}	3863.37 ± 6.03^{b}	4130.74 ± 7.64^{a}

* The CTPSO named for commercial tree peony seed oil, and TPSO-0 and TPSO-15 stand for the oil prepared from ungerminated TPS and germinated for 15 d TPS. Different superscript letters in the same line indicate significant differences ($P < 0.05$), and the data were indicated as mean ± standard deviations (SD).

4. Conclusion

This research determined whether the changes in tissue structure, moisture state of existence and nutritional composition of TPS were related to germination, and further evaluated the nutritional quality of the TPSO. Our study found that the cross-sectional microstructure and oil body structure of TPS were changed after germintated. It mainly includes germination that exposes more fibrous structures and oil amounts, which facilitates the extraction of TPSO. During germination, the water content of TPS increased, primarily due to an increase in the amount of immobilized and free water between cells, and the oil content peaked on the 15th day. Furthermore, the protein and reduced sugar content of TPS increased before decreasing. Also, TPS's protein and reducing sugar content rose and then fell, whereas total sugars was an opposite effect. However, excessive germination may lead to increased lipase activity and energy consumption, thereby accelerating lipid metabolism and reducing overall oil content. Notably, a variety of TPS lipid metabolites were separated and recognized as GL lipids, primarily GL, and containing 48.34% carbon chain unsaturated fatty acids. Subsequent examination revealed significant variations in the TG, DG, PL, PC, SiE, and AcHexSiE classes, suggesting that sprouting significantly altered the lipid profile of TPS. As a result, 15 d after germination, TPSO was prepared. The concentrations of trace lipid concomitants

tocopherols, sterols, and unsaturated fatty acids in germinated TPSO were substantially higher than in the original oil. This study sheds light that germination substantially enhance the nutrient composition and lipid concomitant content of the TPS, making it a economical pretreatment technique for oilseeds. Besides, the research contributes to the selection of TPS with high oil content, and germinated TPS may be more suitable as a raw material for oil of superior nutritional quality. Furthermore, future studies could keep an eye on whether any possible byproducts are created as sprouting techniques are employed on a range of oilseeds.

Acknowledgments

This research was supported by funding from the development of key technologies and products for functional processing and quality preservation of tree peony seed oil (2022GD-TSLD-58-5) and Shaanxi Science and Technology Innovation Team Project (2024RS-CXTD-70). The authors also thank Life Science Research Core Services (LSRCS), Northwest A&F University, for helping with characterization including CLSM (Xiaorui Liu), and SEM (Kerang Huang).

Declaration of competing interest

The authors declare that they have no known competing financial interests or personal relationships that could have appeared to influence the work reported in this paper.

References

[1] Zhang, S., Li, Y., Li, Y., Zhao, F., et al., 2020. Insights on seed abortion (endosperm and embryo development failure) from the transcriptome analysis of the wild type plant species Paeonia lutea. Bioinformation, **16** (8), 638-651.

[2] Deng, R., Gao, J., Yi, J., Liu, P., 2022. Could peony seeds oil become a high-quality edible vegetable oil? The nutritional and phytochemistry profiles, extraction, health benefits, safety and value-added-products. Food Res. Int., **156**, 111200.

[3] Yang, X., Zhang, D., Song, L.M., Xu, Q., et al., 2017. Chemical Profile and Antioxidant Activity of the Oil from Peony Seeds (Paeonia suffruticosa Andr.). Oxidative Med. Cell. Longev., **2017**, 9164905.

[4] Yu, S.Y., Zhang, Y., Lyu, Y.P., Yao, Z.J., et al., 2021. Lipidomic profiling of the developing kernel clarifies the lipid metabolism of Paeonia ostii. Sci. Rep., **11** (1), 12605.

[5] Al-Taher, F., Nemzer, B., 2023. Effect of Germination on Fatty Acid Composition in Cereal Grains. Foods, **12** (17).

[6] Xiang, N., Zhao, Y., Wang, S., Guo, X., 2022. The modulation of light quality on carotenoids in maize (Zea mays L.) sprouts. Food Chem (Oxf), **5**, 100128.

[7] Ohanenye, I.C., Tsopmo, A., Ejike, C.E.C.C., Udenigwe, C.C., 2020. Germination as a bioprocess for enhancing the quality and nutritional prospects of legume proteins. Trends Food Sci. Technol., **101**, 213-222.

[8] Gan, R., Lui, W., Wu, K., Chan, C., et al., 2017. Bioactive compounds and bioactivities of germinated edible seeds and sprouts: An updated review. Trends Food Sci. Technol., **59**, 1-14.

[9] Dong, Y., Wang, N., Wang, S., Wang, J., et al., 2023. A review: The nutrition components, active substances and flavonoid accumulation of Tartary buckwheat sprouts and innovative physical technology for seeds germinating. Front. Nutr., **10**, 1168361.

[10] Ren, X., Xue, J., Wang, S., Xue, Y., et al., 2018. Proteomic analysis of tree peony (Paeonia ostii 'Feng Dan') seed germination affected by low temperature. J. Plant Physiol., **224-225**, 56-67.

[11] Cheng, S., Tang, Y., Zhang, T., Song, Y., et al., 2018. Approach for monitoring the dynamic states of water in shrimp during drying process with LF-NMR and MRI. Dry. Technol., **36** (7), 841-848.

[12] Fu, L., Tan, S., Si, R., Qiang, Y., et al., 2023. Characterization, stability and antioxidant activity of curcumin nanocomplexes with soy protein isolate and pectin. Curr. Res. Food Sci., **6**, 100530.

[13] Garcia, F.L., Ma, S., Dave, A., Acevedo-Fani, A., 2021. Cannabis sativaStructural and Physicochemical Characteristics of Oil Bodies from Hemp Seeds (L.). Foods (Basel, Switzerland), **10** (12).

[14] Dong, Y., Li, Y., Su, W., Sun, P., et al., 2024. Differential metabolic networks in three energy substances of flaxseed (Linum usitatissimum L.) during germination. Food Chem., **443**, 138463.

[15] Wang, X., Li, C., Contreras, M.D., Verardo, V., et al., 2020. Integrated Profiling of Fatty Acids, Sterols and Phenolic Compounds in Tree and Herbaceous Peony Seed Oils: Marker Screening for New Resources of Vegetable Oil. Foods, 9 (6).

[16] Wang, X., Zeng, Q., Verardo, V., Contreras, M.D.M., 2017. Fatty acid and sterol composition of tea seed oils: Their comparison by the "FancyTiles" approach. Food Chem., **233**, 302-310.

[17] Lamont, B.B., 2022. Seed biologists beware: Estimates of initial viability based on ungerminated seeds at the end of an experiment may be error-prone. Plant Biol., **24** (3), 399-403.

[18] Kang, Z.L., Shang, X.Y., Li, Y.P., Ma, H.J., 2022. Effect of ultrasound-assisted sodium bicarbonate treatment on gel characteristics and water migration of reduced-salt pork batters. Ultrason. Sonochem., **89**, 106150.

[19] Wu, J., Li, Y., Gao, X., 2016. Simultaneous determination of oil and water in soybean by LF-NMR relaxometry and chemometrics. Chem. Res. Chin. Univ., **32** (5), 731-735.

[20] Ma, M., Wang, P., Yang, R., Gu, Z., 2018. Effects of UV-B radiation on the isoflavone accumulation and physiological-biochemical changes of soybean during germination: Physiological-biochemical change of germinated soybean induced by UV-B. Food Chem., **250**, 259-267.

[21] Li, T., Tu, C., Rui, X., Gao, Y., et al., 2015. Study of water dynamics in the soaking, steaming, and solid-state fermentation of glutinous rice by LF-NMR: a novel monitoring approach. J. Agric. Food. Chem., **63** (12), 3261-3270.

[22] Guo, L., Wang, H., Hao, C., Chi, Z., et al., 2024. Investigation of the soybean infiltration process utilizing low-field nuclear magnetic resonance technology. PLoS One, **19** (2), e0297756.

[23] Dong, X., Zhang, T., Cheng, S., He, X., et al., 2022. Water and lipid migration in salted duck eggs during storage with different packaging conditions as studied using LF-NMR and MRI techniques. J. Food Sci., **87** (5), 2009-2017.

[24] Konukan, Gozubenli, H., Barutular, C., Hossain, A., et al., 2021. The effects of early harvesting on the seed vigour of three corn (zea mays l.) Hybrids based on germination characteristics. Appl. Ecol. Environ. Res., **19** (2), 1123-1134.

[25] Dong, Y., Tong, C., Li, Q., Zhang, L., et al., 2023. Dynamics of composition, structure, and metabolism of three energy substances in flaxseed (Linum usitatissimum L.) during germination. Food Chem., **410**, 135344.

[26] González-Montemayor, A.M., Solanilla-Duque, J.F., Flores-Gallegos, A.C., López-Badillo, C.M., et al., 2021. Green Bean, Pea and Mesquite Whole Pod Flours Nutritional and Functional Properties and Their Effect on Sourdough Bread. Foods, **10** (9).

[27] Ma, L., Xu, J., Yu, Y., Wang, D., et al., 2023. Effect of high-intensity ultrasound on the structural and functional properties of proteins in housefly larvae (Musca demestica). Ultrason. Sonochem., **101**, 106673.

[28] Kim, E.S., Han, J.H., Olejar, K.J., Park, S.H., 2023. Degeneration of oil bodies by rough endoplasmic reticulum -associated protein during seed germination in Cannabis sativa. AoB Plants, **15** (6), plad082.

[29] Shen, Z.J., Xu, S.X., Huang, Q.Y., Li, Z.Y., et al., 2022. TMT proteomics analysis of a pseudocereal crop, quinoa (Chenopodium quinoa Willd.), during seed maturation. Front. Plant Sci., **13**, 975073.

[30] Zhang, F., Li, Z., Zhou, J., Gu, Y., et al., 2021. Comparative study on fruit development and oil synthesis in two cultivars of Camellia oleifera. BMC Plant Biol., **21** (1), 348.

[31] Liu, Q., Sun, Y., Chen, J., Li, P., et al., 2016. Transcriptome analysis revealed the dynamic oil accumulation in Symplocos paniculata fruit. BMC Genomics, **17** (1), 929.

[32] Li, H., Yue, H., Xie, J., Bu, J., et al., 2021. Transcriptomic profiling of the high-vigour maize (Zea mays L.) hybrid variety response to cold and drought stresses during seed germination. Sci. Rep., **11** (1), 19345.

[33] Zhang, J., Qian, J.Y., Bian, Y.H., Liu, X., et al., 2022. Transcriptome and Metabolite Conjoint Analysis Reveals the Seed Dormancy Release Process in Callery Pear. Int. J. Mol. Sci., **23** (4).

[34] Sánchez-Álvarez, A., Ruíz-López, N., Moreno-Pérez, A.J., Martínez-Force, E., et al., 2019. Agrobacterium-Mediated Transient Gene Expression in Developing Ricinus communis Seeds: A First Step in Making the Castor Oil Plant a Chemical Biofactory. Front. Plant Sci., **10**, 1410.

[35] Bautista-Expósito, S., Vandenberg, A., Peñas, E., Frias, J., et al., 2021. Lentil and Fava Bean With Contrasting Germination Kinetics: A Focus on Digestion of Proteins and Bioactivity of Resistant Peptides. Front. Plant Sci., **12**, 754287.

[36] Gu, J., Hou, D., Li, Y., Chao, H., et al., 2019. Integration of proteomic and genomic approaches to dissect seed germination vigor in Brassica napus seeds differing in oil content. BMC Plant Biol., **19** (1), 21.

[37] Chen, L., Qin, L., Zhang, Y., Xu, H., et al., 2023. Insights from multi-omics integration into seed germination of Taxus chinensis var mairei. Commun. Biol., **6** (1), 931.

[38] Li, S.S., Wang, L.S., Shu, Q.Y., Wu, J., et al., 2015. Fatty acid composition of developing tree peony (Paeonia section Moutan DC.) seeds and transcriptome analysis during seed development. BMC Genomics, **16** (1), 208.

[39] Maia, M., Cavaco, A.R., Laureano, G., Cunha, J., et al., 2021. More than Just Wine: The Nutritional Benefits of Grapevine Leaves. Foods, **10** (10).

[40] Hosni, S., Gani, S., Orsat, V., Hassan, M., et al., 2023. Ultrasound-Assisted Extraction of Antioxidants from Melastoma malabathricum Linn.: Modeling and Optimization Using Box-Behnken Design. Molecules, **28** (2).

[41] Benincasa, P., Falcinelli, B., Lutts, S., Stagnari, F., et al., 2019. Sprouted Grains: A Comprehensive Review. Nutrients, **11** (2).

[42] X, L., S, D., W, B., J, J., et al., 2020. Sesamum indicumMetabolic and transcriptional regulation of phenolic conversion and tocopherol biosynthesis during germination of sesame (L.) seeds. Food Funct., **11** (11), 9848-9857.

[43] Webster, R.D., 2022. Electrochemical and Spectroscopic Characterization of Oxidized Intermediate Forms of Vitamin E. Molecules, **27** (19).

[44] Zhang, X., Zhang, Y., Sun, P., Su, W., et al., 2023. Effect of germination pretreatment on the physicochemical properties and lipid concomitants of flaxseed oil. RSC Adv., **13** (5), 3306-3316.

[45] Liu, R., Lu, M., Zhang, T., Zhang, Z., et al., 2020. Evaluation of the Antioxidant Properties of Micronutrients in Different Vegetable Oils. Eur. J. Lipid Sci. Technol.

[46] Fujita, M., Hasanuzzaman, M., 2022. Approaches to Enhancing Antioxidant Defense in Plants. Antioxidants, **11** (5).